Fabrication of Zn/ZnS nanocable heterostructures by thermal reduction/sulfidation

Quan Li[a] and Chunrui Wang
Department of Physics, The Chinese University of Hong Kong, Shatin, New Territory, Hong Kong, China

(Received 1 November 2002; accepted 15 January 2003)

Single-crystalline Zn/ZnS coaxial nanocables were fabricated through thermal reduction of ZnS using graphite powder at elevated temperatures. Energy dispersive x-ray analysis of the as-fabricated samples indicated that the nanowires were composed of Zn and S only. Transmission-electron-microscopic study of the nanowires revealed that they had core/sheath contrast, suggesting a Zn core/ZnS sheath heterostructure. Epitaxial relationship was observed between the Zn and the ZnS. The possible formation mechanisms of such nanocables are discussed. © *2003 American Institute of Physics.* [DOI: 10.1063/1.1558957]

One-dimensional (1D) nanoscale semiconducting materials have attracted much attention due to their importance in understanding the fundamental roles of dimensionality and quantum size effect, and their potential applications serving as the building blocks for electronic/optical nanodevices.[1–8] Many unique and fascinating properties have been proposed and demonstrated for this class of materials, such as metal–insulator transition,[9] higher luminescence efficiency,[10,11] enhancement of thermoelectric figure of merit,[12] and lowered lasing threshold.[13–15] ZnS was known for a long time as a versatile and excellent phosphor host material. Doped with appropriate ions, a variety of photoluminescent, cathodoluminescent,[16,17] electroluminescent,[18,19] and thermoluminescent[20] properties can be achieved. Among the wide-gap semiconductors, ZnS (band gap 3.7 eV)[21] has a large exciton binding energy (40 meV) and a small Bohr radius (2.4 nm), which make it an excellent candidate in exploring the intrinsic recombination processes in dense excitonic system. This advantage is also expected to be an effective factor for applications in low-threshold ultraviolet lasing.[22–24] Moreover, ZnS is an excellent optical transmissive material due to its broad transmission band (starting from 0.4 μm in the visible to about 14 μm in the infrared region) and the high refractive index value. Inspired by these promising properties and the possible outcome when limiting the ZnS growth within one dimension at the nanometer scale, several groups have fabricated 1D ZnS nanostructures including nanowires,[25] nanorods,[26] and nanotubes[27] recently. In this letter, we report mass production of single crystalline Zn/ZnS nanocables via a thermal reduction route of ZnS by graphite powder. The nanocable is composed of a Zn core and an epitaxial ZnS sheath despite a 43% lattice mismatch between the two. The one-dimensional cable configuration and the epitaxial metal/semiconductor interface may lead to interesting chemical and physical properties unachievable in other nanostructures.

An alumina tube was mounted horizontally inside a high temperature tube furnace. A mixture of 2 g analytical grade ZnS (Goodfellow, 99+%) powder and 2 g graphite (Fisher Chemicals) powder were separately placed on an alumina wafer. The ZnS powder was placed in the center of the alumina tube, and the graphite powder was placed 2 cm downstream the ZnS powder. The tube was then sealed and pumped down to a base pressure of 2×10^{-2} Torr. The furnace was heated up to 800 °C at 10 °C/min, and held at 800 °C for 30 min. The temperature was then further increased to 1300 °C for 5 h before it cools down to room temperature. During the fabrication process, a constant flow of Ar was introduced in the tube at a flow rate of 100 sccm. The total pressure was maintained at 300 mTorr during the growth process. The general morphology and chemical composition of the products were examined by secondary electron microscopy (SEM, LEO 1450 VP) with an energy dispersive x-ray (EDX) spectrometer attached to the microscope. Powder x-ray diffraction (XRD, Rigakau RU-300 with Cu $K\alpha_1$ radiation) was employed to examine the product's overall crystallinity. Detailed microstructure analysis of the products was investigated by transmission electron microscopy (TEM) using a Philips CM 120 microscope operating at 120 kV.

Only graphite powder was left on the alumina boat originally holding ZnS and graphite powder. A dark gray-brownish wool-like material was obtained downstream the alumina tube after the furnace was cooled down to room temperature. XRD pattern of the products is shown in Fig. 1. All the diffraction peaks can be indexed to Zn and ZnS within the experimental error (compared to those of hexago-

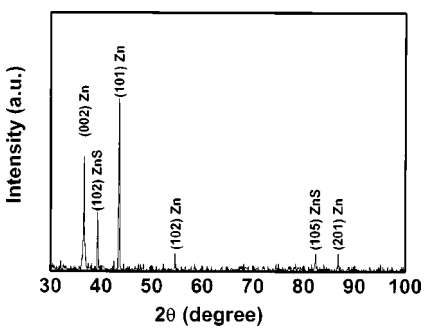

FIG. 1. XRD patterns of as-fabricated products. The diffraction peaks can be indexed to hexagonal Zn and ZnS, as marked on the spectrum.

[a]Author to whom correspondence should be addressed; electronic mail: liquan@phy.cuhk.edu.hk

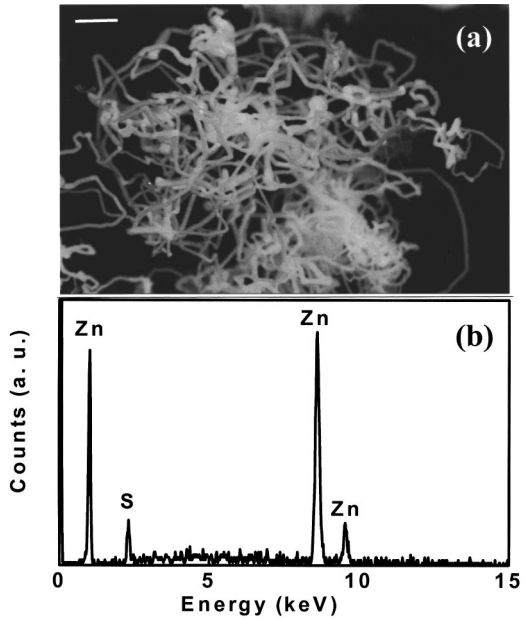

FIG. 2. (a) SEM image reveals the general morphology of the deposited products. Nanowires with uniform diameter (~100 nm) are observed, the scale bar is 100 nm; (b) a typical EDX spectrum taken from single nanowire, suggesting the wire is composed of Zn and S only.

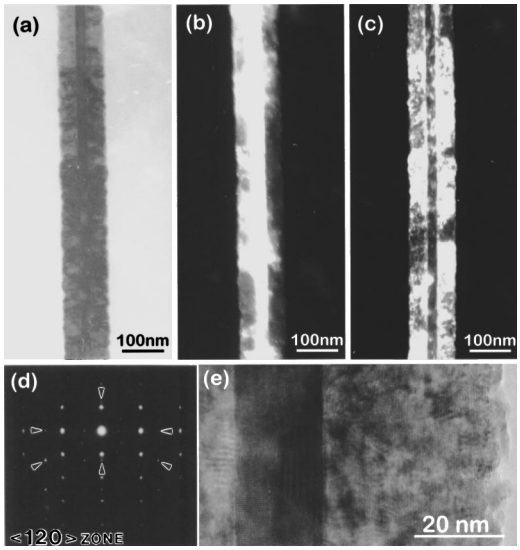

FIG. 3. (a) Low-magnification bright field TEM image of a single nanocable, showing contrast along the cable redial direction; (b) dark field TEM image of the nanocable taken by choosing the Zn$(\bar{2}10)$ diffraction spot; (c) dark field TEM image of the nanocable taken by choosing the ZnS$(\bar{2}10)$ diffraction spot; (d) SAD pattern take from the same nanocable, showing two sets of diffraction spots, corresponding to Zn and ZnS ⟨120⟩ zone, respectively; (e) HREM image of the same nanocable taken with the electron beam along Zn/ZnS ⟨120⟩ zone axis.

nal Zn: $a=2.662$ Å, $c=4.945$ Å and wurtzite ZnS: $a=3.823$ Å, $c=6.261$ Å in the JCPDS files No. 4-831 and 79-2204, respectively).

Figure 2(a) shows a SEM image of the as-fabricated material. The products demonstrate a wire-like morphology. The nanowires appear to be relatively uniform, with an average diameter of ~100 nm, and length up to several tens of microns. EDX was performed on these nanowires. A typical EDX spectrum of a single nanowire is shown in Fig. 2(b), indicating that the nanowire is composed of zinc and sulfur only.

Figure 3(a) gives a low magnification bright field TEM image of such a nanowire. The diameter of the nanowire is ~100 nm, which is consistent with the SEM observation. However, a light/dark/light contrast is observed along the radial direction of the nanowire, suggesting a different phase composition along the wire's radial direction, which leads to the coaxial nanocable structure. TEM observation of several tens of such nanowires reveal that the cable core and sheath thicknesses are not uniform, the core diameters range from 20 to 60 nm and the sheath thicknesses from 40 to 20 nm, respectively. Selected area diffraction pattern (SADP) taken from the nanocable [as shown in Fig. 3(a)] reveals two sets of diffraction spots [Fig. 3(d)], corresponding to those from Zn ⟨120⟩ zone and ZnS ⟨120⟩ zone, respectively. The measured d spacings (from diffraction pattern) of Zn are 2.47 and 1.33 Å, for (002) and $(\bar{2}10)$ planes, respectively. These agree very well with those of hexagonal Zn from the JCPDS file No. 4-831 ($d_{002}=2.47$ Å, $d_{\bar{2}10}=1.33$ Å). The measured d spacings of ZnS are 3.12 and 1.91 Å for (002) and $(\bar{2}10)$ planes, respectively. These match the corresponding d spacings of wurtzite ZnS from the JCPDS file No. 79-2204 ($d_{002}=3.13$ Å, $d_{\bar{2}10}=1.91$ Å). The SADP also suggests an epitaxial relation between the Zn and ZnS with $[120]_{Zn}//[120]_{ZnS}$, $(002)_{Zn}//(002)_{ZnS}$, $(\bar{2}10)_{Zn}//(\bar{2}10)_{ZnS}$.

Figures 3(b) and 3(c) are the dark field TEM images of the same nanocable using a Zn$(\bar{2}10)$ and ZnS$(\bar{2}10)$ diffraction spot, respectively. The light/dark contrast is caused by the diffraction contrast, which indicates that Zn [light in Fig. 3(b), but dark in Fig. 3(c)] and ZnS [light in Fig. 3(c), but dark in Fig. 3(b)] are located in the core and sheath region of the nanocable accordingly. A high-resolution (HR) TEM image of part of the nanocable is shown in Fig. 3(e), which reveals clear core/sheath interface and further confirms the coaxial cable structure. The HREM image was taken with the electron beam along the Zn/ZnS ⟨120⟩ zone axis. Moiré fringes were observed in the cable core region, suggesting the overlapping of two different crystal lattices. The interface between Zn and ZnS is not smooth and possible surface steps exist. The lattice image of the interface is not clearly resolved due to the overlapping of Zn and ZnS crystalline lattice. Nevertheless, a $[120]_{Zn}//[120]_{ZnS}$, $(002)_{Zn}//(002)_{ZnS}$ epitaxial relation can still be observed. The outersurface of the nanocable appears to be rough. Nevertheless, no amorphous material is observed outside the cable surface.

As the products were obtained at the downstream of the alumina tube, the nanocables are formed via a vapor transferring process, namely, the vapor of the nanocable composition material were carried by the processing gas (Ar in this case) and transferred to the downstream of the tube, where the temperature is lower than the center part, and condensed to form nanostructures. As no particle was observed at either end of the nanocable, the vapor–liquid–solid (VLS) mechanism[28] is not appropriate here. Instead, a vapor–solid (VS) mechanism[28] can be used to explain the one-dimensional growth.

The formation of the Zn/ZnS configuration is discussed as following, where carbon is believed to play an important role. ZnS was first reduced to metallic Zn by carbon at high temperature (~1300 °C), which eventually led to the forma-

tion of Zn nanowires. The resulting Zn (bp 907 °C)[29] and CS_2 are in the vapor phase at this temperature. The CS_2 is not stable, it will further decompose into carbon and sulfur, whose process provides the sulfur source. While sulfur (bp 445 °C)[29] will remain in the vapor phase and move with the processing gas Ar, the carbon will be in the solid phase due to its high bp at ~5000 °C,[29] which explains the leftover of the graphite powder on the alumina boat. When the Zn in the vapor phase condenses and grows in the morphology of nanowire[28] at the downstream of the tube where the temperature was lower due to the temperature gradient along tube axis, the surface of the Zn wire reacts with the sulfur and is resulfidized to ZnS, due to the large surface area of Zn wires. Once a thin layer of ZnS is formed outside the Zn nanowire, further ZnS growth (thickening of the sheath) may take over by either S diffusion[30] or Zn and S deposition from the vapor phase.

It is interesting to note that the ZnS sheath is epitaxially grown on zinc, despite a 43% lattice mismatch between the two. Both the Zn and ZnS lattice are completely relaxed, as indicated by the measured d spacings from the nanocable electron diffraction patterns. Although the HREM image is not clear enough to provide any interfacial structural information due to the cable thickness, it is reasonable to speculate that interfacial dislocations must be present to accommodate the large lattice mismatch. It is not clear how the epitaxial relation can be formed under such huge lattice mismatch. Both Zn and ZnS in the presented study preserve hexagonal structure, the geometry similarity between the two lattices may favor the formation of the epitaxial relation. Moreover, if the first ZnS layer on Zn surface was formed by sulfidation of Zn,[30] the resulting orientation of ZnS may be confined by the exposed Zn surface.

In conclusion, Zn/ZnS coaxial nanocables were fabricated via a simple thermal reduction of ZnS using graphite powder. The diameter of the nanocable is ~100 nm. A good epitaxial relation was found between the Zn core and ZnS sheath, despite a 43% lattice mismatch of the two. The nanocable configuration may results from a ZnS reduction followed by Zn sulfidation process. The 1D growth is explained by the VS mechanism as no particle is detected at the end of the nanocables.

This research is supported by RGC direct allocation in the Chinese University of Hong Kong, under Project No. 2060227.

[1] J. Hu, T. W. Odom, and C. M. Lieber, Acc. Chem. Res. **32**, 435 (1999).
[2] C. M. Lieber, Solid State Commun. **107**, 607 (1998).
[3] Y. Cui and C. M. Lieber, Science **291**, 851 (2001).
[4] T. Rueckes, K. Kim, E. Joselerich, G. Y. Tseng, C. Cheung, and C. M. Lieber, Science **289**, 94 (2000).
[5] M. S. Fuhrer, J. Nygard, L. Shih, M. Forero, Y. Yoon, M. S. C. Mazzoni, H. J. Choi, J. Ihm, S. Louie, A. Zettle, and P. L. McEuen, Science **288**, 484 (2000).
[6] S. Noda, K. Tomoda, N. Yamamoto, and A. Chutinan, Science **289**, 604 (2000).
[7] M. Hung, S. Mao, H. Feick, H. Yan, Y. Wu, H. Kind, E. Weberf, R. Russo, and P. Yang, Science **292**, 1897 (2001).
[8] Y. Y. Wu, H. Q. Han, M. Huang, B. Messer, J. B. Song, and P. D. Yang, Chem.-Eur. J. **8**, 1261 (2002).
[9] *Highly Conducting One-Dimensional Solids*, edited by J. T. Devereese, R. P. Evrard, and V. E. van Doren (Plenum, New York, 1979).
[10] L. T. Canham, Appl. Phys. Lett. **57**, 1046 (1990).
[11] J. D. Holmes, K. P. Johnson, R. C. Doty, and B. A. Korgel, Science **287**, 1471 (2000).
[12] L. D. Hicks and M. S. Dresselhaus, Phys. Rev. B **47**, 16631 (1996).
[13] Y. Arakawa and H. Sakaki, Appl. Phys. Lett. **40**, 939 (1982).
[14] Y. Arakawa and A. Yariv, IEEE J. Quantum Electron. **22**, 1887 (1986).
[15] Y. Miyamoto, Y. Miyake, M. Asada, and Y. Suematsu, IEEE J. Quantum Electron. **25**, 2001 (1989).
[16] L. Ozawa, *Cathodoluminescence Theory and Applications* (Kodansha, Tokyo, 1990).
[17] *Phosphor Handbook*, edited by S. Shionoya and W. M. Yen (CRC, Boca Raton, FL, 1999).
[18] J. Valenta, D. Guennani, A. Manar, B. Honerlage, T. Cloitre, and R. L. Aulombard, Solid State Commun. **98**, 695 (1996).
[19] Y. Yamada, T. Yamamoto, S. Nakamura, T. Taguchi, F. Sasaki, S. Kobayashi, and T. Tani, Appl. Phys. Lett. **69**, 88 (1996).
[20] W. Chen, Z. G. Wang, Z. J. Lin, and L. Y. Lin, Appl. Phys. Lett. **70**, 1465 (1997).
[21] R. Menner, B. Dimmler, R. H. Mauch, and H. W. Schock, J. Cryst. Growth **86**, 906 (1988).
[22] J. Valenta, D. Guennani, A. Manar, B. Honerlage, T. Cloitre, and R. L. Aulombard, Solid State Commun. **98**, 695 (1996).
[23] Y. Yamada, T. Yamamoto, S. Nakamura, T. Taguchi, F. Sasaki, S. Kobayashi, and T. Tani, Appl. Phys. Lett. **69**, 88 (1996).
[24] Y. Yamada, in *Optical Properties of Low-Dimensional Materials*, edited by T. Ogawa and Y. Kanemitsu (World Scientific, Singapore, 1995).
[25] X. Jiang, Y. Xie, J. Lu, L. Y. Zhu, W. He, and Y. T. Qian, Chem. Mater. **13**, 1213 (2001); Y. W. Wang, L. D. Zhang, C. H. Liang, G. Z. Wang, and X. S. Peng, Chem. Phys. Lett. **357**, 314 (2002).
[26] D. B. Zhang, L. M. Qi, H. M. Cheng, and J. M. Ma, J. Colloid Interface Sci. **246**, 413 (2002).
[27] L. Dloczik, R. Engelhardt, K. Ernst, S. Fiechter, I. Sieber, and R. Konenkamp, Appl. Phys. Lett. **78**, 3687 (2001).
[28] R. S. Wagner, in *Whisker Technology*, edited by A. P. Levitt (Wiley-Interscience, New York, 1970).
[29] *CRC Handbook of Chemistry Physics* (CRC, Cleveland, OH, 1977).
[30] O. Kubaschewski and B. E. Hopkins, in *Oxidation of Metals and Alloys* (Butterworths, London, 1962).